ELSEVIER

Journal of Nuclear Materials 283–287 (2000) 746–752

journal of nuclear materials

www.elsevier.nl/locate/jnucmat

Statistical analysis of a library of molecular dynamics cascade simulations in iron at 100 K ☆

R.E. Stoller [a,*], A.F. Calder [b]

[a] *Oak Ridge National Laboratory, Metals and Ceramics Division, Bldg. 5500, P.O. Box 2008, Oak Ridge, TN 37831-6376, USA*
[b] *University of Liverpool, Liverpool L693BX, UK*

Abstract

An extensive database of atomic displacement cascades in iron has been developed using molecular dynamics (MD) simulations. Simulations have been carried out at temperatures of 100, 600, and 900 K, and at energies between 0.10 and 50 keV. The results presented here focus on the simulations conducted at 100 K. A sufficient number of cascades has been completed under each condition of cascade energy and temperature to obtain statistically significant average values for the primary damage production parameters. The statistical analysis has been used to examine the influence of primary knockon direction, simulation cell-size, and lattice heating by the high energy recoil. A surprising effect of primary knockon atom (PKA) direction was observed up to 1 keV, but little effect of lattice heating was detected. We have previously reported preliminary results indicating that the ratio of surviving point defects to the number calculated by the Norgett–Robinson–Torrens (NRT) displacement model appears to pass through a minimum value of about 20 keV. The present analysis supports the statistical significance of this minimum, which can be attributed to the onset of extensive subcascade formation.

1. Introduction

Research investigating primary damage formation in metals has made extensive use of molecular dynamics (MD) to simulate atomic displacement cascades and obtain a detailed description of the spatial and temporal extent of these primary damage events [1–14]. Although the method is not new, only recently have modern computers provided the ability to simulate the high energy cascades of primary interest to the fusion materials community. For example, our previous work indicated that subcascade formation should minimize potential differences between fission and fusion irradiation environments [1]. These same computational capabilities have permitted us to assemble an extensive library of atomic displacement cascade simulations in iron. Statistically relevant mean values have been obtained for several primary damage parameters as a function of cascade energy and temperature by conducting a sufficient number of cascades at each condition. The statistical analysis discussed below provides a basis to determine the number of simulations required to obtain meaningful average quantities. The impact of primary knockon atom (PKA) direction and lattice heating induced by the PKA are also discussed. The results presented here focus on simulations conducted at a temperature of 100 K since these comprise the largest component of the database. A similar analysis is being carried out on the 600 and 900 K cascades. These results will be published in the future along with additional details from the 100 K results.

When discussing the energy dependence of defect production, it is convenient to use the number calculated with the standard Norgett–Robinson–Torrens (NRT) secondary displacement model as a normalizing factor [15]. This number of displacements is $\nu_{\mathrm{NRT}} = 0.8T_{\mathrm{dam}}/(2E_{\mathrm{d}})$, where T_{dam} is the so-called damage energy and

☆ Research sponsored at Oak Ridge National Laboratory by the Office of Fusion Energy Sciences and the Division of Materials Sciences, US Department of Energy under contract DE-AC05-96OR22464 with Lockheed Martin Energy Research Corp.

* Corresponding author. Tel.: +1-865 576 788; fax: 1-865 574 0641.

E-mail address: rkn@ornl.gov (R.E. Stoller).

0022-3115/00/$ - see front matter
PII: S0022-3115(00)00074-X

Table 1
Summary of iron cascade database at 100 K

MD cascade energy (keV)	NRT displacements	Number of simulations[a]	Multiple of standard error to be obtained indicated confidence level	
			90%	95%
0.1	1	40	1.685	2.023
0.2	2	32	1.696	2.040
0.3	3	104	1.660	1.983
0.5	5	20	1.729	2.093
1.0	10	12	1.796	2.201
2.0	20	10	1.833	2.262
5.0	50	9	1.860	2.306
10.0	100	15	1.761	2.145
20.0	200	10	1.833	2.262
30.0	300	10	1.833	2.262
40.0	400	8	1.895	2.365
50.0	500	9	1.860	2.306

[a] More simulations have been completed, this is the number used in the average values shown in Fig. 4.

E_d is the average displacement threshold. The damage energy is the portion of the PKA energy that is lost in elastic collisions and can be calculated as described in [15]. Energy lost to electronic excitation and ionization is responsible for the difference between the recoil energy and the damage energy. Since the MD simulations do not account for electronic effects, the MD cascade energy is approximately equivalent to the NRT damage energy. The recommended 40 eV displacement threshold [16] was used to compute the values shown in Table 1.

2. MD simulation method and statistical analysis

All the simulations discussed here were carried out using the MOLDY [17] MD code and the interatomic potential for iron developed by Finnis and Sinclair [18] and subsequently modified by Calder and Bacon [7]. This code and potential have been widely used, and are discussed in detail elsewhere [7,9–14]. Simulations were carried out at constant pressure using periodic boundary conditions. Since the boundary atoms were not damped to remove heat, the kinetic energy of the PKA leads to some lattice heating. This heating has little or no impact on the ballistic phase of the cascade, and the extent to which it may influence the number and configuration of final, stable displacements is not yet clear [14,19]. Some of the results presented below indicate that the effect is not strong.

Typical MD simulation times range from about 5 ps for a 1 keV cascade to more than 15 ps for a 50 keV event. The simulations are terminated when the initial recoil energy has been dissipated and all atomic motion has been thermalized. At this point, the number of stable point defects is counted and their configuration determined. The number of isolated point defects (single interstitials and vacancies) and the number of point defects in clusters are determined as well as the size distributions of vacancy and interstitial clusters. Both the total number of surviving displacements and the fraction of interstitials in clusters will be discussed below, with these parameters presented as a fraction of the NRT displacements.

The results of the cascade simulations have been evaluated using standard statistical methods. From all the simulations at each cascade energy, the mean value (M), the standard deviation about the mean (σ), and the standard error of the mean (ε) have been calculated. The standard error of the mean provides a measure of how well the sample mean is expected to represent the actual mean and is calculated as $\varepsilon = \sigma/n^{0.5}$, where n is the number of simulations completed [20]. Error bars representing confidence levels in a given mean value can be calculated based on ε and n [21] and the error bars can be expressed as a multiple of ε. Table 1 includes these calculated factors for 90% and 95% confidence levels for each set of simulations, where the tabulated n is the total number used to obtain the final set of average values discussed below.

3. Results

Most of the cascade simulations discussed below were generated using a [1 3 5] PKA direction to minimize directional effects such as channeling and directions with particularly low or high displacement thresholds. Our preliminary work indicated that mean values obtained from [1 3 5] cascades should be representative of the average defect production expected in cascades greater than about 1 keV [13]. However, the impact of PKA direction is more significant at lower energies where the

cascade energy is dissipated without involving many atoms and secondary recoil directions. In results published previously [9], we observed that a greater number of simulations was required at the lower energies to obtain average defect production values that varied smoothly with energy. We have conducted many more simulations to further investigate how many are sufficient to yield statistically representative average values. Some of these results are presented in Figs. 1–3. Individual cascade data points are shown, along with their respective average values and error bars indicating the standard error. The data keyed as 'AFC' in these figures are those from the initial studies [7,9]; subsequent data are keyed as 'RES' or 'additional'.

Twelve PKA directions were used in the initial set of sixteen 100, 200, and 300 eV simulations. Subsequently, 24 additional 100 and 300 eV cascades were completed using a [1 3 5] PKA direction and these results are shown in Fig. 1. In the case of the 100 eV cascades in Fig. 1(a), the effect of PKA direction seems relatively modest. The mean values for point defect survival are not significantly different for the two sets of simulations. A third set of 24 [1 1 2] cascades also produced a similar mean survival value. The interstitial clustering fraction was zero for the initial set of 16 simulations, while a few di-interstitials were formed in the set of [1 3 5] and [1 1 2] simulations. A much stronger effect of PKA direction was observed in the case of 300 eV cascades shown in

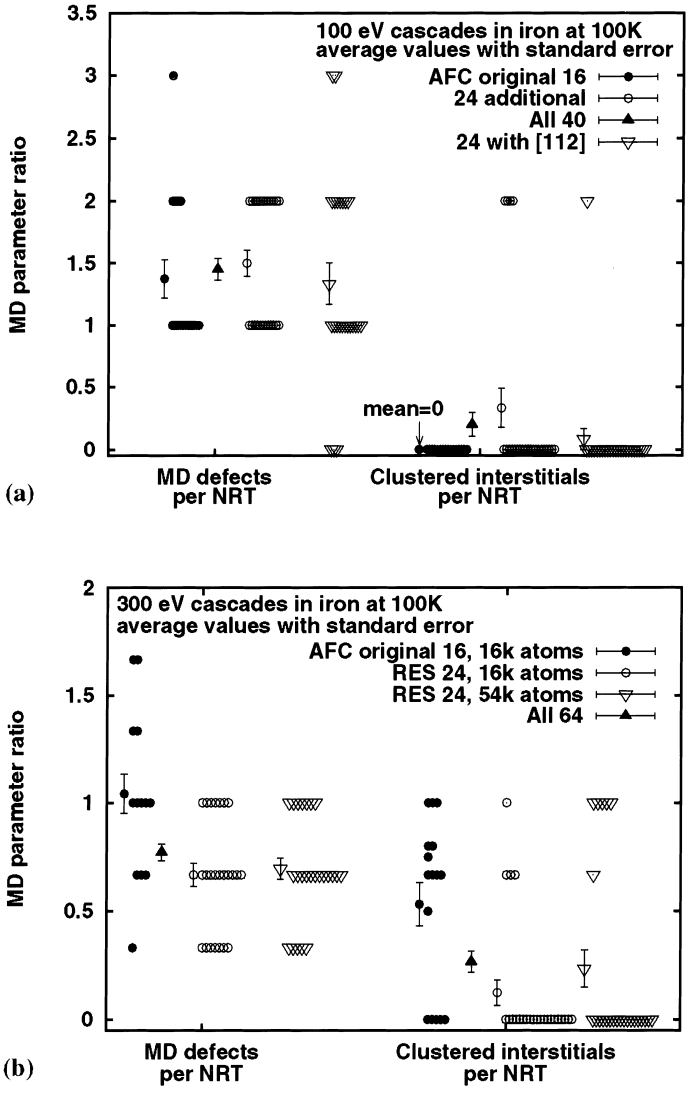

Fig. 1. Results of: (a) 100 eV; (b) 300 eV MD cascade simulations in iron at 100 K.

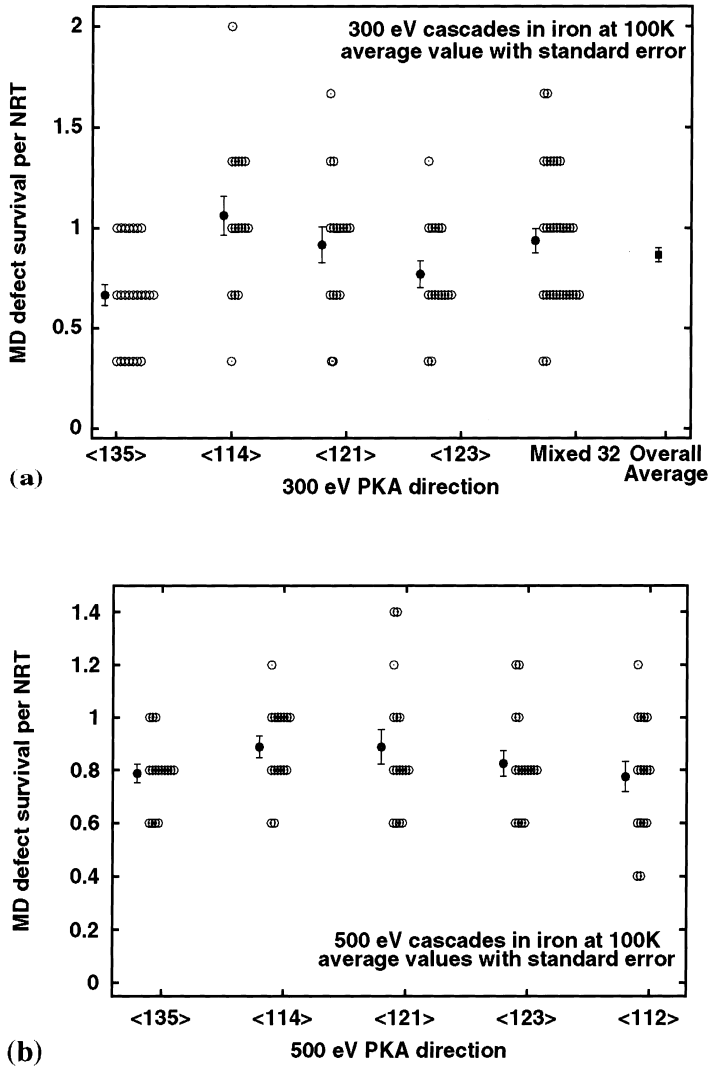

Fig. 2. Impact of PKA direction on displacement production in iron at 100 K from MD cascade simulations at: (a) 300 eV; (b) 500 eV.

Fig. 1(b). The average values obtained from [1 3 5] cascades are plainly not representative of those from the original mix of 12 PKA directions.

The 300 eV simulations were reviewed, and it was determined that PKAs started in [1 1 4] and [1 2 1] directions were primarily responsible for producing the higher average defect survival relative to the [1 3 5] direction. This directional dependence was investigated further and results are summarized in Fig. 2 for 300 and 500 cascades. The unexpected result was that cascades from [1 1 4] and [1 2 1] PKAs exhibited a tendency to be constrained to a single {1 1 0} plane. This planar 'channeling' leads to more efficient separation of vacancies and interstitials. This effect gradually disappears at higher energies as the atomic recoils have a greater probability of breaking out of the plane and generating a three-dimensional cascade. It was surprising to observe that the directional effect persists to some degree up to a cascade energy of 1–2 keV. The ratio of the defect survival using [1 1 4] to that using [1 3 5] was 1.59, 1.12, 1.28, 1.15, and 0.995 for cascade energies of 0.3, 0.5, 1.0, 2.0 and 5.0 keV, respectively.

The first two sets of 16 and 24, 300 eV simulations shown in Fig. 1(b) were carried out using an atom block containing 16 000 atoms. A third set of 24 [1 3 5] simulations was conducted using a 54 000 atom block to demonstrate the effect of lattice heating due to the cascade; these results are also shown in Fig. 1(b). If energy is not removed from the simulation cell, the average temperature increases in proportion to the cascade energy, and decreases linearly with the number of atoms in the cell. In the case of a 300 eV cascade in 16 000 atoms,

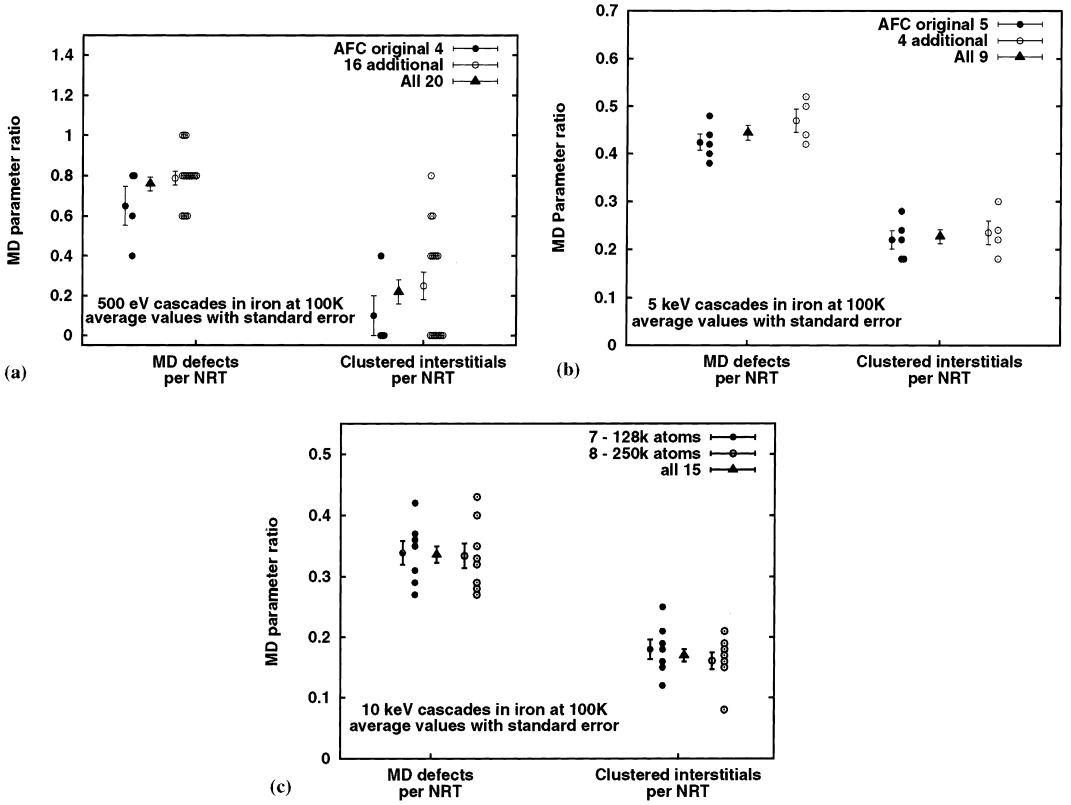

Fig. 3. Results of: (a) 1 keV; (b) 5 keV; (c) 10 keV MD cascade simulations in iron at 100 K.

a temperature rise of about 72 K is obtained once the energy has been dissipated. For a 54 000 atom block, this temperature rise is reduced to 22 K. The defect survival fraction is essentially unchanged as a result of this lattice heating, but the average interstitial clustering fraction is slightly higher in the larger (cooler) atom block.

The results of 0.5, 5, and 10 keV simulations are shown in Fig. 3, where the original 4,5, and 7 simulations have been supplemented by 16, 4, and 8 additional simulations, respectively. The 500 eV results clearly indicate that four simulations are not sufficient for determining the average defect survival at this energy, while the two sets of simulations at 5 keV show less dispersion. When compared with the data shown in Fig. 1, this indicates a trend toward fewer simulations being required as the cascade energy increases. The 10 keV results shown in Fig. 3(c) also provide a second example of the effect of simulation cell size. The average defect survival values are virtually identical for the two sets of simulations, seven in a 128 000 atom block and eight in a 250 000 atom block. A very slight decrease in interstitial clustering is observed in the larger (cooler) atom block. This variation is not statistically significant. Taken together, the two sets of 10 keV results suggest that about 8–10 simulations are sufficient to obtain representative average values at this energy.

The energy dependence of stable defect formation observed in the MD cascade database is summarized in Fig. 4, where three distinct energy regimes can be observed. Defect formation in each of these regions can be characterized by a simple power law. In a broad region between 0.5 and 20 keV, the number of defects produced increases with an exponent of about 0.75 as first reported by Bacon et al. [11]. The number of defects produced at lower and higher energies is greater than that predicted by an extrapolation of this equation. Greater defect survival is expected at lower energies where true cascade conditions do not occur and relatively isolated point defect pairs are produced. The increase above 20 keV is associated with subcascade formation, and increasing separation between subcascades at the highest energies. The regions between subcascades are characterized by relatively low energy collisions with a higher probability of defect survival. The small standard errors (nearly indistinguishable from the data points) shown in Fig. 4 provide statistical support for the greater than linear energy dependence shown in the figure. If the data in Fig. 4 are normalized

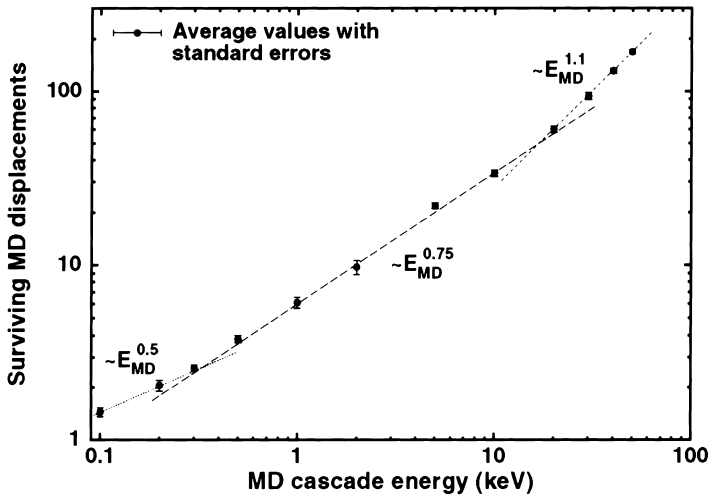

Fig. 4. Number of surviving displacements in iron MD cascade simulations at 100 K, error bars showing standard error are nearly obscured by size of data points.

using the NRT displacements, the curve of defect survival fraction exhibits a minimum near 20 keV [14].

4. Discussion and conclusions

The data indicate that some dependence on PKA direction persists up to 1 keV. For the PKA directions used in this work, the maximum difference in defect survival occurred when comparing the [1 3 5] and [1 1 4] directions, due to an unexpected planar channeling observed with [1 1 4]. The difference between the [1 3 5] and [1 1 4] averages are statistically significant at the 95% confidence level for the 0.3 keV simulations, but not at higher energies. For example, although the [1 1 4] defect survival was 15% higher than [1 3 5] at 2 keV, this difference is not statistically significant at the 90% confidence level. These results suggest the necessity of conducting low-energy simulations in a variety of high and low index directions to characterize defect survival before choosing a single direction for high energy simulations. It is interesting to note that PKA directions which gave higher than average survival were not necessarily directions with a low displacement threshold [22]. Interstitial clustering appears to be somewhat less sensitive to PKA direction than does defect survival.

Using 40 simulations and 12 PKA directions yielded a standard error equal to 6% of the average defect survival at 100 eV. A similar value of 8.7% was obtained from the initial 16 simulations and 12 directions at 300 eV. There is a trend indicating that fewer simulations are required at higher energies, e.g., the standard-error-to-average ratio is 6.5% with 12 simulations at 1 keV, less than 5% with 10 simulations at 20 and 30 keV and as low as 2.5% with 9 simulations at 50 keV.

Gao et al. [19] developed a hybrid MD model to extract heat from the simulation block in order to investigate the effect of lattice heating by the PKA. Their results suggest that there is little effect of heating on defect survival, but a possibly significant impact on interstitial clustering at elevated temperatures. The comparison presented above for 0.3 and 10 keV cascades are based simply on using larger atom blocks to reduce the heating. Defect survival is unchanged, while interstitial clustering is slightly greater in the cooler block at 0.3 keV and slightly lower in the cooler block at 10 keV. The change is not statistically significant in either case at the 90% confidence level. Gao et al. reported a reduction in clustering for 5 keV cascades at 100 K that is somewhat larger than our result at 10 keV.

Finally, the results of this analysis confirm an effect of subcascade formation that we have previously reported [1]. The ratio of surviving point defects to the number calculated by the NRT displacement model passes through a minimum value of about 20 keV, and the statistical significance of this minimum seems established. The increase above this value is reflected in the change in slope of the defect survival curve at 20 keV in Fig. 4. The reason for the increase appears to be related to the spacing between the subcascades at higher energies. Inspection of the cascades indicates that point defects created in regions between subcascades have a higher probability of survival because the defect density in these regions is relatively low, similar to low energy cascades. These regions of higher defect survival occur with greater frequency at the high energies, giving rise to

the greater than linear energy dependence. Initial analysis of a limited number of 100 keV cascade suggests that this effect may be saturating.

Although the validity of these results has only been demonstrated for the particular iron potential employed in this work, they should provide useful guidance for investigations of primary damage formation in other materials. A more complete analysis of the iron cascade database will be published when a set of 100 keV cascades has been completed and the 600 and 900 K simulations have been fully analyzed.

Acknowledgements

The authors appreciate helpful discussions with Dr S.J. Zinkle of ORNL. Research sponsored by the Office of Fusion Energy Sciences and the Division of Materials Sciences, US Department of Energy and the Office of Nuclear Regulatory Research, US Nuclear Regulatory Commission under interagency agreement DOE 1886-N695-3W with the US Department of Energy, under contract DE-AC05-84OR21400 with Lockheed Martin Energy Research, Corp.

References

[1] R.E. Stoller, L.R. Greenwood, J. Nucl. Mater. 271&272 (1999) 57.
[2] K. Morishita, T. Diaz de la Rubia, J. Nucl. Mater. 271&272 (1999) 35.
[3] J.B. Gibson, A.N. Goland, M. Milgram, G.H. Vineyard, Phys. Rev. 120 (1960) 1229.
[4] R.S. Averback, T. Diaz de la Rubia, R. Benedek, Nucl. Instrum. and Meth. B 33 (1988) 693.
[5] T. Diaz de la Rubia, M.W. Guinan, J. Nucl. Mater. 174 (1990) 151.
[6] A.J.E. Foreman, W.J. Phythian, C.A. English, Philos. Mag. A 66 (1992) 571.
[7] A.F. Calder, D.J. Bacon, J. Nucl. Mater. 207 (1993) 25.
[8] D.J. Bacon, T. Diaz de la Rubia, J. Nucl. Mater. 216 (1994) 275.
[9] W.J. Phythian, R.E. Stoller, A.J.E. Foreman, A.F. Calder, D.J. Bacon, J. Nucl. Mater. 223 (1995) 245.
[10] R.E. Stoller, in: I.M. Robertson, L.E. Rehn, S.J. Zinkle, W.J. Phythian (Eds.), Microstructure of Irradiated Materials. Symp. Proc. vol. 373, Materials Research Society, Warrandale, PA, 1995, p. 21.
[11] D.J. Bacon, A.F. Calder, F. Gao, V.G. Kapinos, S.J. Wooding, Nucl. Instrum. and Meth. B 102 (1995) 37.
[12] R.E. Stoller, J. Nucl. Mater. 233–237 (1996) 999.
[13] R.E. Stoller, G.R. Odette, B.D. Wirth, J. Nucl. Mater. 251 (1997) 49.
[14] R.E. Stoller, J. Nucl. Mater. 276 (1999) 22.
[15] M.J. Norgett, M.T. Robinson, I.M. Torrens, Nucl. Eng. Des. 33 (1975) 50.
[16] ASTM E521,Standard Practice for Neutron Radiation Damage Simulation by Charged-Particle Irradiation, Annual Book of ASTM Standards, vol. 12.02, American Society of Testing and Materials, West Conshohocken, PA.
[17] M.W. Finnis, MOLDY6-A Molecular Dynamics Program for Simulation of Pure Metals, AERE R-13182, UK AEA Harwell Laboratory, 1988.
[18] M.W. Finnis, J.E. Sinclair, Philos. Mag. A 50 (1984) 45; Erratum, Philos. Mag. A 53 (1986) 161.
[19] F. Gao, D.J. Bacon, P.E.J. Flewitt, T.A. Lewis, J. Nucl. Mater. 249 (1997) 77.
[20] A. Stuart, J.K. Ord, Kendall's Advanced Theory of Statistics, vol. 1, Charles Griffin and Company, London, 1987.
[21] Manual on Presentation of Data and Chart Control Analysis, sixth ed., American Society for Testing and Materials, West Conshohocken, PA, 1992.
[22] D.J. Bacon, A.F. Calder, J.M. Harder, S.J. Wooding, J. Nucl. Mater. 205 (1993) 52.